Recessive mutation in tetraspanin *CD151* causes Kindler syndrome-like epidermolysis bullosa with multi-systemic manifestations including nephropathy

Hassan Vahidnezhad[a,b,1], Leila Youssefian[a,c,1], Amir Hossein Saeidian[a], Hamidreza Mahmoudi[d], Andrew Touati[a,e], Maryam Abiri[f], Abdol-Mohammad Kajbafzadeh[g], Sophia Aristodemou[h], Lu Liu[h], John A. McGrath[i], Adam Ertel[j], Eric Londin[j], Ariana Kariminejad[k], Sirous Zeinali[b], Paolo Fortina[j,l] and Jouni Uitto[a,m]

***a* - Department of Dermatology and Cutaneous Biology,** *Sidney Kimmel Medical College, Thomas Jefferson University, Philadelphia, PA, USA*
***b* - Molecular Medicine Department,** *Biotechnology Research Center, Pasteur Institute of Iran, Tehran, Iran*
***c* - Department of Medical Genetics,** *School of Medicine, Tehran University of Medical Sciences, Tehran, Iran*
***d* - Department of Dermatology,** *Razi Hospital, Tehran University of Medical Sciences, Tehran, Iran*
***e* - Drexel University College of Medicine,** *Philadelphia, PA, USA*
***f* - Department of Medical Genetics and Molecular Biology,** *School of Medicine, Iran University of Medical Sciences, Tehran, Iran*
***g* - Pediatric Urology Research Center,** *Department of Urology, Children's Hospital Medical Center, Tehran University of Medical Sciences, Tehran, Iran*
***h* - Viapath,** *St Thomas' Hospital, London, UK*
***i* - Department of Medical and Molecular Genetics,** *St. John's Institute of Dermatology, King's College London (Guy's Campus), London, UK*
***j* - Computational Medicine Center,** *Sidney Kimmel Cancer Center, Thomas Jefferson University, Philadelphia, PA, USA*
***k* - Kariminejad-Najmabadi Pathology & Genetics Center,** *Tehran, Iran*
***l* - Department of Molecular Medicine,** *Sapienza University, Rome, Italy*
***m* - Jefferson Institute of Molecular Medicine,** *Thomas Jefferson University, Philadelphia, PA, USA*

Correspondence to Jouni Uitto: *Department of Dermatology and Cutaneous Biology, Sidney Kimmel Medical College, Thomas Jefferson University, 233 S. 10th Street, Suite 450 BLSB, Philadelphia, PA 19107, USA. Jouni.Uitto@Jefferson.edu*
https://doi.org/10.1016/j.matbio.2017.11.003

Abstract

Epidermolysis bullosa (EB) is caused by mutations in as many as 19 distinct genes. We have developed a next-generation sequencing (NGS) panel targeting genes known to be mutated in skin fragility disorders, including tetraspanin *CD151* expressed in keratinocytes at the dermal-epidermal junction. The NGS panel was applied to a cohort of 92 consanguineous families of unknown subtype of EB. In one family, a homozygous donor splice site mutation in *CD151* (NM_139029; c.351 + 2T > C) at the exon 5/intron 5 border was identified, and RT-PCR and whole transcriptome analysis by RNA-seq confirmed deletion of the entire exon 5 encoding 25 amino acids. Immunofluorescence of proband's skin and Western blot of skin proteins with a monoclonal antibody revealed complete absence of CD151. Transmission electron microscopy showed intracellular disruption and cell-cell dysadhesion of keratinocytes in the lower epidermis. Clinical examination of the 33-year old proband, initially diagnosed as Kindler syndrome, revealed widespread blistering, particularly on pretibial areas, poikiloderma, nail dystrophy, loss of teeth, early onset alopecia, and esophageal webbing and strictures. The patient also had history of nephropathy with proteinuria. Collectively, the results suggest that biallelic loss-of-function mutations in *CD151* underlie an autosomal recessive mechano-bullous disease with systemic features. Thus, *CD151* should be considered as the 20th causative, EB-associated gene.

Introduction

Complexity of the basement membranes

Basement membranes comprise of complex networks of interacting matrix macromolecules separating epithelia from the underlying mesenchymal tissues where they play physiologically important roles [1]. In the skin, the dermal-epidermal basement membrane is responsible for stable adhesion of epidermis to the underlying dermis [2,3]. The presence of distinct basement membrane components, their appropriate supramolecular assembly and their macromolecular interactions are critical for the functional integrity of these structures. While most basement membranes universally consist of the principal components, such as type IV collagen, laminin-111 and heparin sulfate proteoglycans, certain basement membranes have characteristic protein components in a restricted tissue distribution critical for their specialized tissue-specific function. For example, in the skin, hemidesmosomes, critical attachment complexes, consist of type XVII collagen, α6β4 integrin and tetraspanin CD151 [4,5]. The hemidesmosomes connect the intermediate filament network, consisting of keratins 5 and 14 in the intracellular milieu of basal keratinocytes, to anchoring filaments, extracellular filamentous structures which traverse lamina lucida and consist primarily of laminin-332. On the dermal side of the cutaneous basement membrane zone, anchoring fibrils, comprised of type VII collagen, stabilize the association of lamina densa to the underlying dermis [6]. The contiguous network of hemidesmosomes, anchoring filaments and anchoring fibrils is required for stable association of the epidermis to the underlying dermis.

Phenotypic and genotypic heterogeneity of epidermolysis bullosa

Mutations in the cutaneous basement membrane zone genes can result in fragility of the skin, which as a result of minor trauma leads to blistering and erosions. The prototype of such heritable skin fragility disorders is epidermolysis bullosa (EB), currently known to be associated with mutations in as many as 19 distinct genes [7–10]. The topographic level of expression of these EB-associated genes within the basement membrane zone, the types and combinations of mutations and their consequences at the mRNA and protein levels, when juxtaposed to environmental factors, primarily external trauma, result in considerable phenotypic heterogeneity noted in this group of disorders. In addition to cutaneous findings, some forms of EB are associated with extracutaneous manifestations in the ocular, gastrointestinal, pulmonary, and vesico-urinary systems [11]. Combinations of skin fragility and extracutaneous manifestations can lead to considerable morbidity and in some cases early mortality.

The tetraspanin family of proteins

Tetraspanins consist of a superfamily of transmembrane proteins widely distributed on a variety of cell types, and they have been implicated in a broad spectrum of cellular processes under physiological conditions [12]. Specifically, tetraspanins form specialized membrane microdomains on the cell surface controlling cell proliferation and migration, angiogenesis and adhesion. The expression of various tetraspanins has also been shown to be associated with a number of different human malignancies with pathomechanistic roles as well as serving as prognostic markers [13,14]. Tetraspanin CD151 is widely distributed in different tissues, including epithelium, endothelium, muscle, renal glomeruli and proximal and distal tubules [15]. This protein is also expressed in the epidermis and has been shown to be a component of the hemidesmosomes [4,5]. Tetraspanin CD151 is an endogenous component of basement membranes in the skin, in hemidesmosomes and focal adhesions, where it forms stable laminin-binding complexes with α3β1 and α6β4 integrins, as well as in the kidneys where it interacts with α3β1 and α6β1 integrins [16]. CD151 is a 253-amino acid protein with a single N-glycosylation site, and immunoblotting reveals bands of apparent molecular weights of 28 and 32 kDa representing unglycosylated and glycosylated forms, respectively [17].

We have developed a next generation sequencing (NGS) panel covering 21 skin fragility-associated genes, including *CD151*, which was used to screen for pathogenic sequence variants in EB. In this study, we report a patient with a homozygous splice site mutation in *CD151* resulting in deletion of exon 5 corresponding to a transmembrane domain, associated with multi-system involvement, including skin fragility with a Kindler syndrome-like phenotype (Fig. 1).

Results

Next generation sequencing identifies a homozygous donor splice site mutation in *CD151*

We have developed a targeted NGS array covering 21 genes associated with skin fragility disorders, specifically consisting of 18 genes previously shown to harbor mutations in different forms of EB [7]. Three additional genes that are not in the current classification of EB but which are associated with inherited skin fragility and therefore in the differential diagnosis of EB were included: *CDSN* and *CHST8*, associated with peeling skin syndromes, as well as *CD151* which has

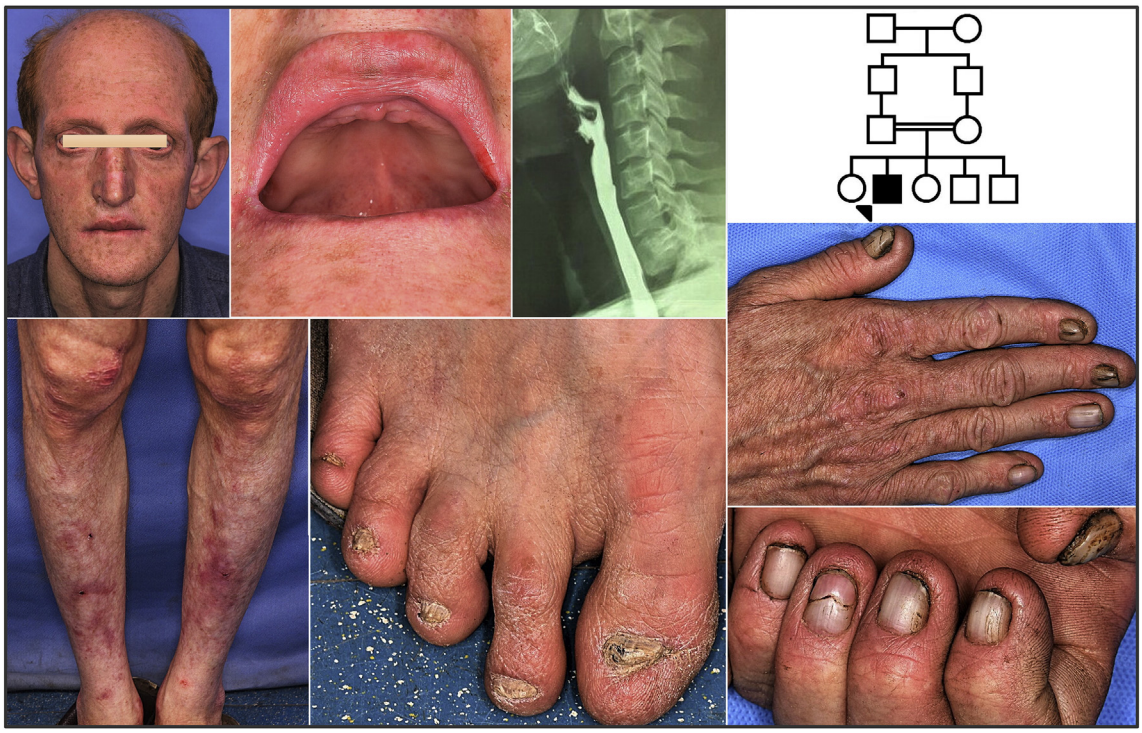

Fig. 1. Clinical features of the proband with Kindler syndrome-like phenotype. Note facial freckling, loss of teeth, pretibial blistering, nail dystrophy, and atrophy of the back of the hands. The patient also had esophagus webbing and strictures. The patient is the only affected individual in the consanguineous family with first cousin parents.

been previously reported to have mutations with complex nephropathy and blistering phenotype (for the list of all genes in the panel, see Materials and Methods). The sequencing panel was applied to DNA from 92 probands, each representing a distinct family, with the clinical diagnosis of EB, based on history of neonatal blistering and erosions of the skin. NGS, followed by extensive bioinformatics analysis, identified in one proband a homozygous mutation, NM_139029:c.351 + 2T>C, in *CD151* affecting the canonical donor splice site junction sequence, AG/gt at the exon 5/intron 5 border (Fig. 2a). This mutation was predicted to result in aberrant splicing affecting exon 5. The presence of this mutation at the genomic level was confirmed by PCR, followed by bi-directional Sanger sequencing (Fig. 2c), and the patient's parents were shown to be heterozygous carriers of this mutation. Homozygosity mapping showed an ~10 Mb run of homozygosity (ROH) harboring *CD151* on chromosome 11 (p.15.5-p.15.4).

Consequences of the *CD151* mutation at transcriptome level

To examine the consequences of the mutation at transcriptional level and also to exclude other possible mutations throughout the exome, RT-PCR and independently whole transcriptome sequencing (RNA sequencing, RNA-seq) of mRNA isolated from a skin biopsy were performed. Sanger sequencing of RT-PCR product spanning exons 4–6 revealed the deletion of a segment of sequences corresponding to exon 5 and consisting of 75 nucleotides, indicating that the deletion was in-frame (Fig. 2c).

Recently, the potential utility of whole transcriptome sequencing for clinical genetic evaluation of Mendelian disorders was demonstrated in *COL6A1* muscular dystrophy and *TIMMDC1* mitochondrial complex I deficiency cohorts [18,19]. We performed RNA-seq scanning of whole transcriptome of our case, and the results confirmed skipping of exon 5 of *CD151*. A Sashimi plot was generated to visualize and quantify the consequences of this splicing abnormality, which identified a splicing event utilizing the donor splicing site of exon 4 and the acceptor splicing site of exon 6 in 91 out of 92 transcriptional reads (Fig. 2b). The deleted sequence of the mRNA encodes a segment of 25 amino acids in positions 93–117 of the CD151, which by modeling was shown to include the third transmembrane segment within the EC2 domain of the protein (Fig. 3a).

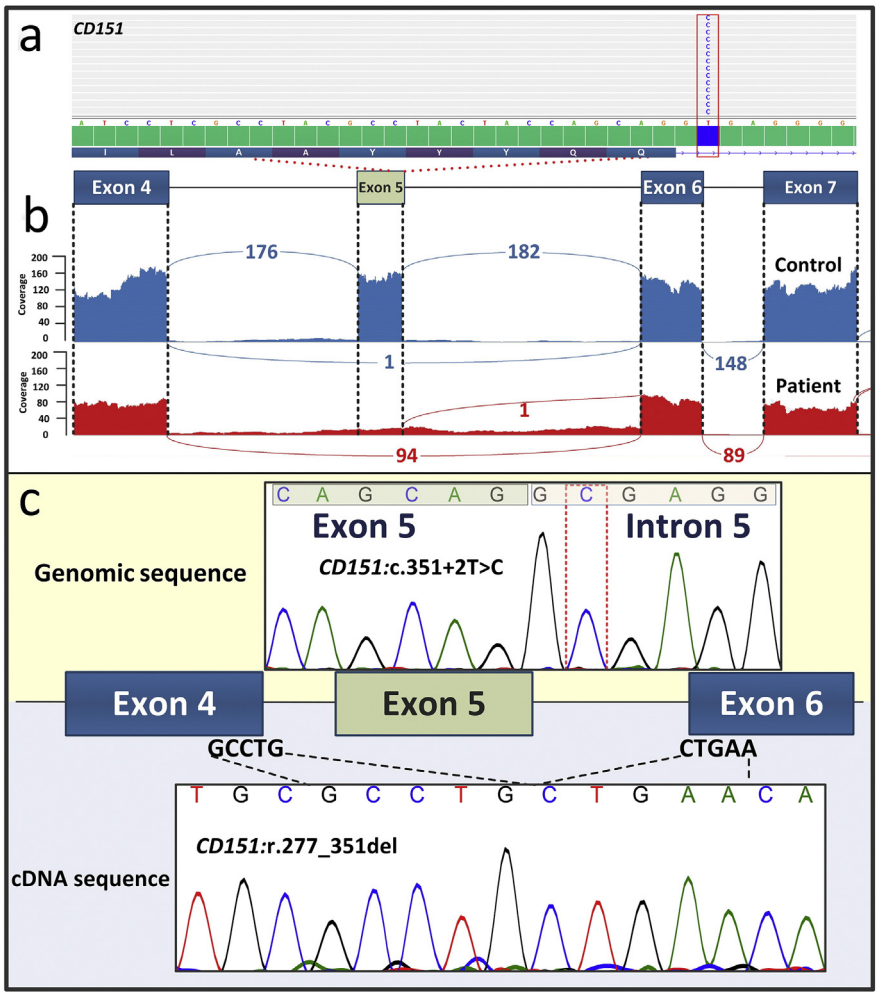

Fig. 2. Next generation sequencing reveals a homozygous splice-site mutation in the *CD151* gene. (a) Screen shot of the genomic sequence visualized by the Integrative Genomics Viewer demonstrating homozygous T-to-C transition mutation which resides in *CD151* within the canonical splice-site sequence AG/gt at the exon 5/intron 5 border. (b) Sashimi plot of RNA-seq reveals that the *CD151* mutation results in skipping of the entire exon 5 consisting of 75 bp (lower panel, red), as compared to splicing in control RNA (upper panel, blue). (c) The mutation was confirmed at the genomic level by Sanger sequencing (upper panel), as well as at the cDNA level by RT-PCR using mRNA isolated from the patient's skin sample as template (lower panel).

Consequences of the mutation at protein and ultrastructural levels

To examine the consequences of the mutation at protein level, immunofluorescence of the patient's skin was performed with a monoclonal anti-CD151 antibody. The specificity of this antibody was confirmed by Western analysis which identified a band of ~28 kDa with protein isolated from control skin samples (Fig. 3d). Parallel staining of control skin from an unaffected, unrelated individual revealed strong linear staining at the dermal-epidermal junction with some of the staining extending to the lateral surfaces of the basal keratinocytes (Fig. 3b). In contrast, immunostaining with the same antibody was completely negative in the patient's skin, indicating the absence of the epitope recognized by this antibody (Fig. 3c). Western blot of protein isolated from a biopsy from the patient's skin showed absence of *CD151* (Fig. 3d).

Transmission electron microscopy of the patient's skin showed both intracellular and intercellular disruption and dysadhesion (Fig. 3e). Some cells showed keratin filament aggregation and cytolysis, and there was widening of spaces between some cells with poor desmosomal connections. There was an apparent increase in intercellular accumulation of electron dense material and cellular debris. Hemidesmosomes appeared somewhat small with impaired keratin filament association. In contrast, anchoring fibrils below the lamina densa were

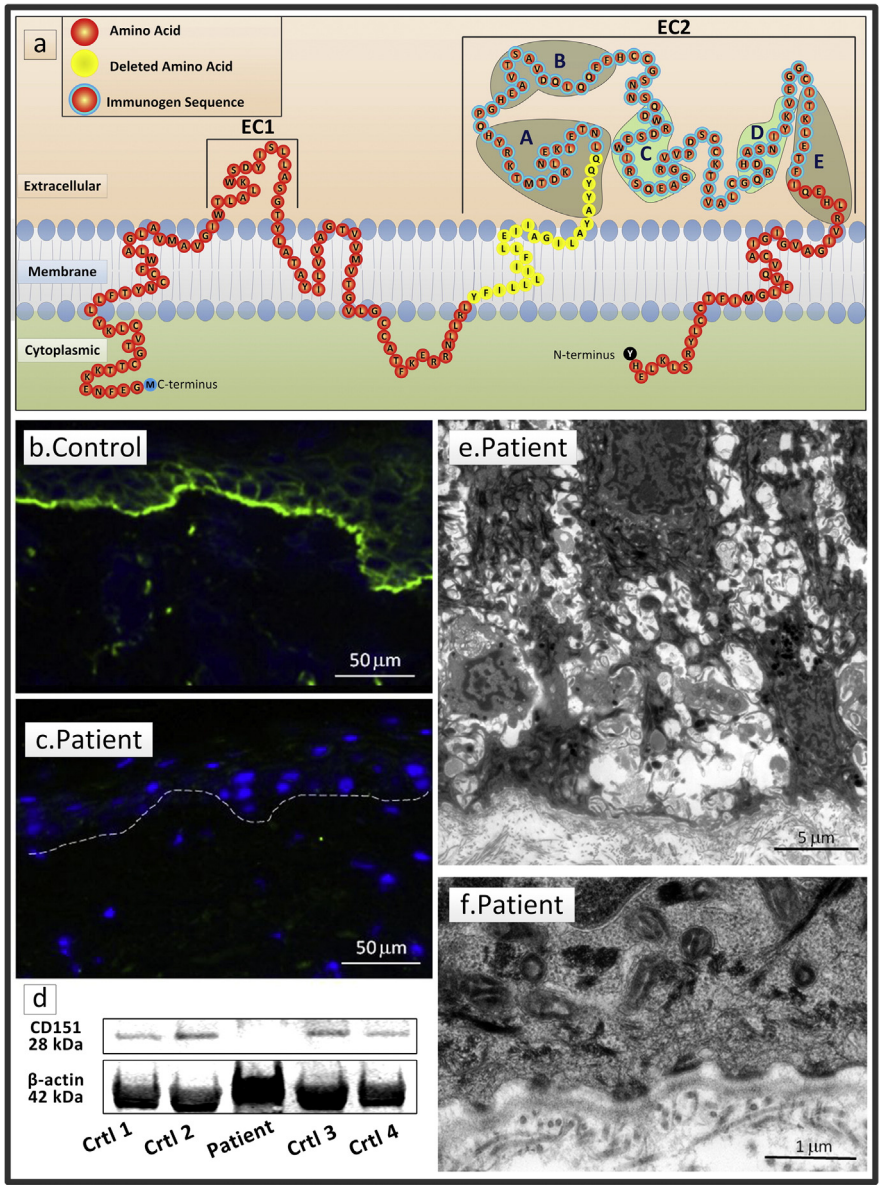

Fig. 3. Consequences of mutation at protein and ultrastructural level. (a) The 253-amino acid tetraspanin CD151 protein consists of four transmembrane domains and two extracellular loops (EC1, EC2). The EC2 contains specific regions involved in homodimerization (A, B and E) and in interactions with other proteins, such as integrins (C and D). The deleted 25-amino acid peptide segment of CD151 (yellow amino acids) includes the third transmembrane spanning domain. The amino acids included in the immunogen used for development of the monoclonal antibody used in this study are designated by a blue rim. (b) Immunostaining of control skin with an anti-CD151 monoclonal antibody reveals linear staining of the dermal-epidermal junction which extends to the lateral sides of basal keratinocytes. (c) Staining of the patient's skin with the same antibody was entirely negative. The dashed line indicates the position of the basement membrane zone. The sections were counterstained with DAPI (blue). (d) Western blot analysis of protein isolated from skin biopsies from four age-matched controls (Ctrl 1–4) with a monoclonal antibody to CD151 reveals a band of 28 kDa, while the patient's skin biopsy is devoid of CD151 protein (upper panel). Reprobing of the filter, after stripping, with an antibody to β-actin reveals an abundance of protein as represented by the 42 kDa band (lower panel). (e) Transmission electron microscopy of the patient's skin demonstrates intracellular and intercellular disruption and dysadhesion of basal keratinocytes. There is widening of spaces between some cells with poor desmosomal connections. (f) Higher magnification reveals accumulation of electron dense material and cellular debris. Hemidesmosomes appear somewhat small with impaired keratin filament association, but anchoring fibrils are numerous and display normal ultrastructural features.

numerous and displayed normal ultrastructural features (Fig. 3f).

Clinical features of the proband

The 33-year old proband with a homozygous *CD151* mutation was referred to this study with a clinical diagnosis of Kindler syndrome (KS). He was the only affected individual in the family with evidence of consanguinity in a first-cousin marriage (Fig. 1). Clinical examination of the proband revealed features of KS with phenotypic overlap with some forms of junctional EB, generalized intermediate, including facial freckling, poikiloderma and atrophy of the skin and acrogeria of the backs of the hands on the sun-exposed areas. He had widespread blistering and erosions primarily in the pretibial area but also scattered on other parts of the body, particularly those exposed to trauma. He also had erosions in the oral mucous membranes. He was completely edentulous and had anamnestically lost all teeth by around 16 years of age (Fig. 1). The patient had dystrophic nails in all fingers and toes, and had early-onset alopecia. He had corneal vascularization and symptomatic nasolacrimal duct stenosis. He also had a history of difficulty with swallowing, and barium radiography revealed esophageal webbing and strictures (Fig. 1). The patient had history of nephropathy manifesting with proteinuria (for detailed clinical description, see Case Report in Supplementary Material).

Discussion

Epidermolysis bullosa is a phenotypically heterogeneous condition with highly variable severity. EB was initially divided into three broad categories, *viz.*, simplex, junctional and dystrophic subtypes, based on the topographic level of tissue separation within the cutaneous basement membrane zone [7]. More recently, Kindler syndrome with neonatal blistering has been added as the fourth major type of EB [20,21]. The phenotypic variability in EB reflects, to a large part, genetic heterogeneity, and as many as 19 distinct genes expressed at the dermal-epidermal basement membrane zone have been shown to harbor mutations in different variants of EB [8,10]. The demonstration of mutations in the *CD151* gene brings this number to 20. The mutation reported in this study leads to aberrant splicing of exon 5 and deletion of 25 amino acids from the CD151 protein, with profound consequences to the ultrastructure of basal keratinocytes, including disintegration and dysadhesion. Since no blistering was noted in the skin samples used for immunofluorescence, it was not possible to determine what distinct major category of EB the CD151 deficiency belongs to. However, considering the facts that the ultrastructural changes in this patient were somewhat similar to those noted in patients with mutations in the *EXPH5* gene, a form of EB simplex [22], and that *CD151* is expressed in the basal keratinocytes [23], one could classify inherited CD151 pathology as an EB simplex variant. Immunofluorescence and Western blot analysis of the patient's skin showed complete absence of immunostaining. The precise epitope of the monoclonal antibody, which was commercially available, is unknown, but the immunogenic peptide used for development of this antibody (Leu118-Phe215) resides just outside of the deleted region in CD151 (see Fig. 3a), and it is therefore likely that the absent immunofluorescence staining in the patient's skin reflects the absence of the protein which may have become unstable as a result of the mutation.

The patient was referred to our laboratory for genetic testing with the diagnosis of KS. His clinical features were consistent with this diagnosis included poikiloderma, facial freckling and acrogeria, as well as skin blistering which was more severe during childhood and became more moderate in the adulthood. Considering the diagnosis of KS, the *FERMT1* gene was first sequenced by Sanger technique but no pathogenic sequence variants were found. A characteristic ultrastructural feature of KS is blistering within multiple levels of the dermal-epidermal adhesion zone which results in reduplication of the cutaneous basement membrane. The latter feature was not evident in ultrastructural examination by transmission electron microscopy, further suggesting subclassification of this case as a form of EB simplex with KS-like clinical features. It should also be noted that the proband had esophageal webbing and strictures, features consistently associated with the recessive dystrophic subtype of EB, but also reported in KS [24]. Moreover, the clinical features also showed some overlap with generalized intermediate junctional EB [7]. Thus, the proband has some KS-like features but the overall clinical findings indicate a distinct clinicopathologic entity.

Our patient has clinical similarities to three MER2-negative patients in two families of Indian Jewish origin with end-stage renal disease (ESRD) with a homozygous indel mutation c.383insG in *CD151* causing a frame-shift and premature stop codon (See Table 1) [25]. In addition to hereditary nephritis, two of these patients had sensorineural deafness, nasolacrimal duct stenosis and β-thalassemia minor, as well as pretibial EB. The authors concluded that CD151 is essential for the proper assembly of the glomerular and tubular basement membrane in kidney, has functional significance in the skin, is probably a component of the inner ear, and could play a role in erythropoiesis [25]. In our patient, there was no evidence of sensorineural deafness, and analysis of hemoglobin showed no evidence of β-thalassemia. The fragility of skin in our patient was more severe and extended from pretibial area to other parts of the body

Table 1. Comparison of pertinent phenotypic characteristics of the index patient in this report with those of the patients in a previous report of *CD151*-associated disease. The findings present in these patients are also compared to those findings generally associated with different types of epidermolysis bullosa[a].

Clinical manifestations	Present report	Previous report[b]	Categories of EB typically associated with finding
Cutaneous			
Blistering over bony prominences	+ (Extensive)	+ (Pretibial)	DDEB-pt., RDEB-pt. [7]
Poikiloderma	+	N/A	KS [21]
Nail dystrophy	+	+	EBS, JEB, DEB, KS [7]
Alopecia	+	N/A	JEB, RDEB [7]
Ocular			
Ectropion	+	N/A	JEB-gs, RDEB-gs, KS [38]
Nasolacrimal duct stenosis	+	+	JEB, RDEB [39]
Oral			
Oral mucosal involvement	+	N/A	EBS-gs, JEB, DEB, KS [7]
Microstomia	+	N/A	JEB-gs, RDEB, KS [40]
Dystrophic teeth	+ (Edentulous)	+	JEB, RDEB [11]; KS [21]
Gastrointestinal			
Esophageal involvement	+ (Webbing and strictures)	N/A	JEB-gs [21], DEB [41], KS [21]
Gastroesophageal reflux	+	N/A	EBS-gs, JEB, RDEB [41]
Malnutrition	+	N/A	JEB, RDEB [7], KS [21]
Constipation	+	N/A	DEB [42], KS [20]
Renal			
Protein-wasting nephropathy	+	+ (ESRD)	JEB-rri [29], JEB-PA [43], RDEB [44]
Genitourinary			
Distal vaginal agenesis	N/A	+	Not reported
Urinary incontinence	+	N/A	JEB, RDEB [41]; KS [21]
Other			
Anemia	–	+ (BT minor)	JEB-gs [7], RDEB [7], KS [7]
Sensorineural hearing loss	– (4 kHz notch)	+	RDEB [41]

[a] Abbreviations: N/A = information not available or not applicable; ESRD = End-stage renal disease; BT minor = Beta thalassemia minor; EBS = Epidermolysis bullosa simplex; JEB = Junctional epidermolysis bullosa; DEB = Dystrophic epidermolysis bullosa; KS = Kindler syndrome; DDEB-pt. = Dominant DEB pretibial; RDEB-pt. = Recessive DEB, pretibial; EBS-gs = EBS, generalized severe; JEB-gs = JEB, generalized severe; RDEB-gs = RDEB, generalized severe; JEB-rri = JEB with respiratory and renal involvement; JEB-pa = JEB with pyloric atresia.
[b] Karamatic Crew et al., 2004.

subject to trauma (see Case Report in Supplementary Material). Our patient had, however, renal disease which was less severe than that in previously reported MER2-negative cases which developed ESRD. These phenotypic differences might reflect differences in the mutations and their consequences or may result from genetic and environmental modifying factors. Thus, the combination of overlapping findings with inter-patient variability calls for identification of additional patients with CD151 deficiency to further elucidate genotype-phenotype correlations towards understanding of the *CD151* associated disease in the EB spectrum (Table 1).

The pathomechanistic details by which the exon-skipping mutation in *CD151*, delineated in our study, are likely to involve interactions with laminin-binding integrins expressed within the basement membrane zones. Specifically, CD151 has been demonstrated to associate with integrins α3β1, α6β1, α6β4 and α7β1 in cells in culture and *in vivo* [16]. Several model systems have revealed that binding of CD151 with these receptors, particularly with α3β1, strengthens their association with laminins. The association of CD151 with α3β1 integrin has been shown to be regulated by glycosylation of this laminin receptor, with consequent changes in cell spreading, motility, degradation and integrity of basement membranes [26]. The protein sequences mediating association of CD151 with α3β1 integrin map within the large extracellular loop EC2 which spans the amino acid residues Tyr112-Leu220, a region mostly outside of the deleted segment in the mutant CD151 in our patient. However, various deletions within the protein, particularly involving the small extracellular loop and transmembrane domains, including the third transmembrane domain deleted in the mutant protein in our patient, prevent surface expression of CD151 mutants, and the mutant protein accumulates in the rough endoplasmic reticulum and is then redirected to the lysosomes [27]. Thus, the absence of immunofluorescence staining with the CD151 antibody used in our study may reflect degradation of the mutant protein. CD151 associates with α3β1 as well as by α6β4 integrin in the formation of mature hemidesmosomes of the cutaneous basement membrane, where this tetraspanin likely plays a role in hemidesmosomal stability [28]. As a consequence of a loss of functional CD151, compromised interactions between laminin-332 and both α3β1 and α6β4 integrin would result in perturbations in basement membrane stability and a reduced functional capacity as a layer stabilizing the association of the epidermis to the underlying dermis. This basement

membrane pathology then results in a form of EB, manifesting with blistering and erosions as a result of trauma, as is evident in our proband. In support of this notion are demonstrations that patients with homozygous mutations in the *ITGA3* gene encoding the integrin α3 subunit result in disrupted basement membrane structures and compromised barrier functions in kidney, lung and skin, leading to multi-organ disorder that includes congenital nephrotic syndrome, interstitial lung disease, and EB [29]. In these patients the renal and respiratory features predominate, and the lung involvement accounts for the lethal course of the disease at the early age.

The mechanisms by which CD151 deficiency results in kidney failure have been examined in *Cd151*-null mice that recapitulate the renal pathology noted in human patients [30,31]. These mice developed proteinuria caused by focal glomerular sclerosis, disorganization of the glomerular basement membranes, and tubular cystic dilatation. Furthermore, generation of podocyte-specific conditional knockout mice for the integrin α3 subunit showed renal defects similar to those in *Cd151* knockout mice. These observations support the overall conclusions that CD151 plays a key role in strengthening adhesion of keratinocytes mediated laminin-α3β1 integrin complex in the epidermis and podocytes in the renal tissue, resulting in a distinct phenotype of EB with multi-system involvement, as observed in our patient.

The classification of EB continues to be evaluated, refined and expanded with status updates published in a series of international consensus reports [7,32,33]. Over time, several new clinicopathologic entities have been incorporated to the formal classification of EB, notably with several new subtypes of EB simplex being added in recent years. Although the most recent classification from 2014 lists 18 candidate genes [7], a 19th gene, *KLHL24*, has been widely accepted for inclusion following a series of cases reported in 2016 and 2017 [9,10,34,35]. However, a number of other genes/skin fragility disorders reside on the fringes of the classification, not yet absorbed into the mainstream listing. Our data here provide strong justification for inclusion of *CD151* officially as the 20th gene in the classification of EB.

Materials and methods

Targeted next generation sequencing

DNA from 92 probands of families with unspecified forms of EB was extracted from peripheral blood samples taken from patients, their parents and other clinically affected and unaffected family members using a QIAamp DNA Blood Mini Kit (Qiagen, Valencia, CA). This study was approved by the Institutional Review Board of the Pasteur Institute of Iran, and all subjects as well as parents of underage patients gave written informed consent to participate in research and gave their permission to publish their images. DNA was examined with a Qubit 2.0 fluorometer (Life Technologies, Carlsbad, CA) for concentration and quality. Target enrichment was performed using TruSeq Custom Amplicon Kit (Illumina Inc., San Diego, CA). The sequencing library was designed by DesignStudio (Illumina Inc.), and contained 21 genes (*CD151*, *CDSN*, *CHST8*, *COL17A1*, *COL7A1*, *DSP*, *DST*, *EXPH5*, *FERMT1*, *ITGA3*, *ITGA6*, *ITGB4*, *JUP*, *KRT5*, *KRT14*, *LAMA3*, *LAMB3*, *LAMC2*, *PKP1*, *PLEC1*, and *TGM5*) divided into 421 targets covered by 968 amplicons. This array covered all coding exons, at least 20 bp of the flanking intronic sequences at the intron-exon borders, and up to 50 bp of 5'- and 3′-untranslated regions of these genes. The amplicon panel was designed to cover 99% of the targeted bases, and a total of 36,724,892 reads were aligned to the human genome. The mean coverage of the target region was 424×. DNA from the probands, together with an Illumina control, were multiplexed using dual indexing with 12 primary indexes and 8 secondary indexes. Dual indexed samples were normalized to be equimolar and pooled together following manufacturer's recommendations. The pool of 96 samples was sequenced on a single MiSeq flow-cell (Illumina Inc.). DNA fragments were sequenced using paired-end 225-nt reads using dual indexes, which generated 8.94 Gbp. The reads were aligned to the Human Genome version GRCh38 using the Burrows-Wheeler Alignment (BWA) Tool BWA-MEM algorithm. Prior to variant calling, GATK tools RealignerTargetCreator, IndelRealigner, BaseRecalibrator, and PrintReads were used to preprocess the aligned reads with local realignments and base quality score recalibration for optimized accuracy. Single nucleotide variants and insertions/deletions were called using the Bayesian genetic variant analysis tool FreeBayes [https://arxiv.org/abs/1207.3907].

Single nucleotide variants and insertion/deletions were annotated using ANNOVAR software, which includes data from the 1000 genomes project, ClinVar, dbSNP, and dbNSFP, a database of human non-synonymous SNPs and their functional predictions based on combined SIFT, Polyphen2, LRT, and MutationTaster scores. Variants were initially filtered to exclude loci with fewer than 5 supporting reads or alternate allele fraction <0.25. Homozygous variants were then prioritized for pathogenicity starting with nonsense mutations followed by large deletions, frameshift insertions/deletions, canonical splice sites, and finally nonsynonymous point mutations with deleterious effects as documented in ClinVar or predicted by dbNSFP. In those samples without homozygous deleterious mutation candidates, genes were further analyzed for compound heterozygous

mutations comprising combinations of two or more events including nonsense mutations, frameshift insertions/deletions, canonical splice sites, and non-synonymous point mutations.

Pathogenicity of identified variants was designated according to the American College of Medical Genetics Standards, and sequence variants were classified either as pathogenic, likely pathogenic, or of unknown significance [36]. Population allele frequencies were determined using the Exome Aggregation Consortium (Exac.broadinsitute.org), the 1000 Genomes database (1000genomes.org), and GnomAD (Gnomad.broadinsitute.org). The pathogenic/likely pathogenic variants were confirmed by sequencing of both alleles by Sanger sequencing. PCR was performed using Taq polymerase (Qiagen), and the products were bi-directionally sequenced using an automated sequencer (AB3730; Applied Biosystems, Foster City, CA, USA).

RNA extraction, cDNA synthesis, RT-PCR, PCR and Sanger sequencing

Biopsied skin samples from the patient were immediately placed in Invitrogen™ RNAlater™ Stabilization Solution and transferred to the laboratory for extraction of RNA using TRIzol® Reagent (Ambion, Life Technologies). One µg of DNase-treated total RNA was reverse transcribed (SuperScript III First Strand Synthesis System, Invitrogen # 18080–051) using gene-specific and universal primers followed by RNase H treatment to degrade the RNA. 2 µl of the reverse transcription reaction mixture was used for PCR reaction using a *CD151* specific primer encompassing the exons 4–6. Polymerase Chain Reaction (PCR) was performed using Taq polymerase (Qiagen) according to the manufacturer's instructions. The RT-PCR products were bi-directionally sequenced using an automated sequencer (AB3730; Applied Biosystems). In addition, exonic regions and their flanking intronic sequences harboring pathogenic variants which were captured by NGS panel of EB associated genes were amplified and sequenced using newly designed primers (sequences available upon request), spanning all exons and ~50 bp of the flanking intronic sequences.

RNAseq

Total RNA was extracted from a skin biopsy obtained from the proband using TRIzol® Reagent and quantified on a Nanodrop ND-100 spectrophotometer (Thermo Fisher Scientific, Wilmington, DE), followed by RNA quality assessment on an Agilent 2200 TapeStation (Agilent Technologies, Palo Alto, CA). Multiplexed library construction, workflow analysis and sequencing runs were performed following standard Illumina protocols (Illumina, Inc., San Diego, CA) using the TruSeq Stranded Total RNA kit with indexes from Set A (Cat #: RS-122-2301). Paired-end (2 × 75) sequencing reads were generated on the Illumina NextSeq 500 platform and stored in FASTQ format. TruSeq RNA adapter sequences were trimmed from the reads prior to alignment. Reads were aligned using STAR 2-Pass version 2.5.2b [37] with the human genome version hg38 as the reference genome and GENCODE V24 annotations. Only reads mapping uniquely to the genome were maintained. During the mapping, a first-pass alignment was performed to identify the discovery of unannotated junctions. These junctions were then used to create a new annotation file for the second-pass alignment as recommended by the STAR manual to enable sensitive junction discovery.

Immunofluorescence staining and Western analysis

For immunofluorescence, skin sections (5 µm) were air-dried and initially blocked with diluted normal goat serum (Sigma-Aldrich, Dorset, UK), and then incubated with anti-CD151 (clone ab33315, 11G5a, Abcam, Cambridge, UK) diluted 1:10 in phosphate-buffered saline with 30% *w/v* bovine serum albumin (Sigma-Aldrich). After washing in phosphate-buffered saline, slides were labeled with fluorescein isothiocyanate secondary antibodies (Invitrogen, Paisley, UK). Negative controls omitting the primary antibody were also performed. All sections were photographed using the same camera and identical exposure times (3 s).

For Western analysis, skin biopsy samples from the patient and normal healthy individuals were collected and homogenized by sonication in lysis buffer. The protein concentrations were determined using the Qubit Protein assay kit (ThermoFisher, Waltham, Massachusetts, USA). Equal amounts of total protein (80 µg) were loaded onto 4–20% gradient gels for electrophoresis, followed by transfer to polyvinylidene difluoride membranes. Membranes were blocked in 5% milk followed by incubation with the primary polyclonal rabbit anti-human antibody for HPA011906 CD151 at 1:1000 (Sigma Aldrich, MO, USA) with a secondary goat anti-rabbit antibody 925-32211 (LI-COR, Lincoln, Nebraska USA) at 1:15,000. The housekeeping protein beta-actin was analyzed using the primary monoclonal mouse anti-human antibody ab8224 at 1:20,000 (Abcam, Cambridge, MA, USA) with a secondary goat anti-mouse 926-32210 at 1:20,000 (LI-COR). Membranes were visualized using the Odyssey CLx near-infrared fluorescence imaging system (LI-COR).

Transmission electron microscopy

Skin biopsy specimens were cut into small pieces (<1 mm^3) and fixed in half-strength Karnovsky fixative for 4 h at room temperature. After washing in 0.1 M phosphate buffer (pH 7.4), the samples

were immersed in 1.3% aqueous osmium tetroxide (TAAB Laboratories, Berkshire, UK) for 2 h, followed by incubation in 2% uranyl acetate (Bio-Rad, Hertfordshire, UK), and dehydrated in a graded ethanol series, and then embedded in epoxy resin *via* propylene oxide (TAAB Laboratories). Ultra-thin sections were stained with uranyl acetate and lead citrate and examined in a Philips CM10 transmission electron microscope (Philips, Eindhoven, The Netherlands).

Acknowledgments

The authors thank Sara Norouz-zadeh, Sara Afsharaalam and Hamideh Bagherian for assistance in collection and processing of the samples and the clinical data. Tina Hashemi and Jefferson medical students Yael Horvath, Megan O'Donnell and Kathryn Sommers assisted in Western blot analysis. Carol Kelly assisted in manuscript preparation. This work was supported by DEBRA International (JU). This study is in partial fulfillment of the PhD Thesis of HV.

Appendix A. Supplementary data

Supplementary data to this article can be found online at https://doi.org/10.1016/j.matbio.2017.11.003.

Received 11 August 2017;
Received in revised form 3 November 2017;
Accepted 3 November 2017
Available online 11 November 2017

Keywords:
Epidermolysis bullosa;
Kindler syndrome;
Nephropathy;
CD151;
Next generation sequencing;
RNA-seq;
Tetraspanin CD151

[1]These authors contributed equally to this work.

Abbreviations used:
EB, epidermolysis bullosa; NGS, next generation sequencing; KS, Kindler syndrome.

References

[1] A. Pozzi, P.D. Yurchenco, R.V. Iozzo, The nature and biology of basement membranes, Matrix Biol. (2017) 1–11 57-58.
[2] C. Has, L. Bruckner-Tuderman, The genetics of skin fragility, Annu. Rev. Genomics Hum. Genet. 15 (2014) 245–268.
[3] J. Uitto, C. Has, H. Vahidnezhad, L. Youssefian, L. Bruckner-Tuderman, Molecular pathology of the basement membrane zone in heritable blistering diseases: the paradigm of epidermolysis bullosa, Matrix Biol. (2017) 76–85 57-58.
[4] L. Nahidiazar, M. Kreft, B. van den Broek, P. Secades, E.M. Manders, A. Sonnenberg, K. Jalink, The molecular architecture of hemidesmosomes, as revealed with super-resolution microscopy, J. Cell Sci. 128 (20) (2015) 3714–3719.
[5] G. Walko, M.J. Castanon, G. Wiche, Molecular architecture and function of the hemidesmosome, Cell Tissue Res. 360 (3) (2015) 529–544.
[6] H.J. Chung, J. Uitto, Type VII collagen: the anchoring fibril protein at fault in dystrophic epidermolysis bullosa, Dermatol. Clin. 28 (1) (2010) 93–105.
[7] J.D. Fine, L. Bruckner-Tuderman, R.A. Eady, E.A. Bauer, J.W. Bauer, C. Has, A. Heagerty, H. Hintner, A. Hovnanian, M.F. Jonkman, I. Leigh, M.P. Marinkovich, A.E. Martinez, J.A. McGrath, J.E. Mellerio, C. Moss, D.F. Murrell, H. Shimizu, J. Uitto, D. Woodley, G. Zambruno, Inherited epidermolysis bullosa: updated recommendations on diagnosis and classification, J. Am. Acad. Dermatol. 70 (6) (2014) 1103–1126.
[8] J. Uitto, H. Vahidnezhad, L. Youssefian, Genotypic heterogeneity and the mode of inheritance in epidermolysis bullosa, JAMA Dermatol. 152 (2016) 517–520.
[9] J.Y.W. Lee, L. Liu, C.K. Hsu, S. Aristodemou, L. Ozoemena, M. Ogboli, C. Moss, A.E. Martinez, J.E. Mellerio, J.A. McGrath, Mutations in KLHL24 add to the molecular heterogeneity of epidermolysis bullosa simplex, J. Invest. Dermatol. 137 (6) (2017) 1378–1380.
[10] C. Has, The "Kelch" surprise: KLHL24, a new player in the pathogenesis of skin fragility, J. Invest. Dermatol. 137 (6) (2017) 1211–1212.
[11] J.D. Fine, J.E. Mellerio, Extracutaneous manifestations and complications of inherited epidermolysis bullosa: part II. Other organs, J. Am. Acad. Dermatol. 61 (3) (2009) 387–402.
[12] S.J. van Deventer, V.E. Dunlock, A.B. van Spriel, Molecular interactions shaping the tetraspanin web, Biochem. Soc. Trans. 45 (3) (2017) 741–750.
[13] H.M. Romanska, F. Berditchevski, Tetraspanins in human epithelial malignancies, J. Pathol. 223 (1) (2011) 4–14.
[14] P. Zeng, Y.H. Wang, M. Si, J.H. Gu, P. Li, P.H. Lu, M.B. Chen, Tetraspanin CD151 as an emerging potential poor prognostic factor across solid tumors: a systematic review and meta-analysis, Oncotarget 8 (3) (2017) 5592–5602.
[15] M.E. Hemler, Tetraspanin functions and associated microdomains, Nat. Rev. Mol. Cell Biol. 6 (10) (2005) 801–811.
[16] L.M. Sterk, C.A. Geuijen, J.G. van den Berg, N. Claessen, J.J. Weening, A. Sonnenberg, Association of the tetraspanin CD151 with the laminin-binding integrins alpha3beta1, alpha6beta1, alpha6beta4 and alpha7beta1 in cells in culture and in vivo, J. Cell Sci. 115 (Pt 6) (2002) 1161–1173.
[17] N.V. Whittock, W.H. McLean, Genomic organization, amplification, fine mapping, and intragenic polymorphisms of the human hemidesmosomal tetraspanin CD151 gene, Biochem. Biophys. Res. Commun. 281 (2) (2001) 425–430.
[18] B.B. Cummings, J.L. Marshall, T. Tukiainen, M. Lek, S. Donkervoort, A.R. Foley, V. Bolduc, L.B. Waddell, S.A. Sandaradura, G.L. O'Grady, E. Estrella, H.M. Reddy, F. Zhao, B. Weisburd, K.J. Karczewski, A.H. O'Donnell, D. Luria, A. Birnbaum, Y. Hu Sarkozy, H. Gonorazky, K. Claeys,

H. Joshi, A. Bournazos, E.C. Oates, R. Ghaoui, M.R. Davis, N.G. Laing, A. Topf, C. Genotype-Tissue Expression, P.B. Kang, A.H. Beggs, K.N. North, V. Straub, J.J. Dowling, F. Muntoni, N.F. Clarke, S.T. Cooper, C.G. Bonnemann, D.G. MacArthur, Improving genetic diagnosis in Mendelian disease with transcriptome sequencing, Sci. Transl. Med. 9 (386) (2017).

[19] L.S. Kremer, D.M. Bader, C. Mertes, R. Kopajtich, G. Pichler, A. Iuso, T.B. Haack, E. Graf, T. Schwarzmayr, C. Terrile, E. Konarikova, B. Repp, G. Kastenmuller, J. Adamski, P. Lichtner, C. Leonhardt, B. Funalot, A. Donati, V. Tiranti, A. Lombes, C. Jardel, D. Glaser, R.W. Taylor, D. Ghezzi, J.A. Mayr, A. Rotig, P. Freisinger, F. Distelmaier, T.M. Strom, T. Meitinger, J. Gagneur, H. Prokisch, Genetic diagnosis of Mendelian disorders via RNA sequencing, Nat. Commun. 8 (2017) 15824.

[20] J.E. Lai-Cheong, J.A. McGrath, Kindler syndrome, Dermatol. Clin. 28 (1) (2010) 119–124.

[21] L. Youssefian, H. Vahidnezhad, A. Hossein Saeidian, K. Ahmadizadeh, C. Has, J. Uitto, Kindler syndrome, an orphan disease of cell/matrix adhesion in the skin - molecular genetics and therapeutic opportunities, Expert Opin. Orphan Drugs 4 (2016) 845–854.

[22] J.A. McGrath, K.L. Stone, R. Begum, M.A. Simpson, P.J. Dopping-Hepenstal, L. Liu, J.R. McMillan, A.P. South, C. Pourreyron, W.H. McLean, A.E. Martinez, J.E. Mellerio, M. Parsons, Germline mutation in EXPH5 implicates the Rab27B effector protein Slac2-b in inherited skin fragility, Am. J. Hum. Genet. 91 (6) (2012) 1115–1121.

[23] S.M. Geary, A.J. Cowin, B. Copeland, R.M. Baleato, K. Miyazaki, L.K. Ashman, The role of the tetraspanin CD151 in primary keratinocyte and fibroblast functions: implications for wound healing, Exp. Cell Res. 314 (11 – 12) (2008) 2165–2175.

[24] A. Ohashi, Y. Kiniwa, R. Okuyama, T. Kosho, T. Suga, C. Has, H. Kubo, A case of Kindler syndrome with severe esophageal stenosis, Int. J. Dermatol. 54 (4) (2015) e106–8.

[25] V. Karamatic Crew, N. Burton, A. Kagan, C.A. Green, C. Levene, F. Flinter, R.L. Brady, G. Daniels, D.J. Anstee, CD151, the first member of the tetraspanin (TM4) superfamily detected on erythrocytes, is essential for the correct assembly of human basement membranes in kidney and skin, Blood 104 (8) (2004) 2217–2223.

[26] A. Ranjan, S.M. Bane, R.D. Kalraiya, Glycosylation of the laminin receptor (alpha3beta1) regulates its association with tetraspanin CD151: impact on cell spreading, motility, degradation and invasion of basement membrane by tumor cells, Exp. Cell Res. 322 (2) (2014) 249–264.

[27] F. Berditchevski, E. Gilbert, M.R. Griffiths, S. Fitter, L. Ashman, S.J. Jenner, Analysis of the CD151-alpha3beta1 integrin and CD151-tetraspanin interactions by mutagenesis, J. Biol. Chem. 276 (44) (2001) 41165–41174.

[28] L.M. Sterk, C.A. Geuijen, L.C. Oomen, J. Calafat, H. Janssen, A. Sonnenberg, The tetraspan molecule CD151, a novel constituent of hemidesmosomes, associates with the integrin alpha6beta4 and may regulate the spatial organization of hemidesmosomes, J. Cell Biol. 149 (4) (2000) 969–982.

[29] C. Has, G. Sparta, D. Kiritsi, L. Weibel, A. Moeller, V. Vega-Warner, A. Waters, Y. He, Y. Anikster, P. Esser, B.K. Straub, I. Hausser, D. Bockenhauer, B. Dekel, F. Hildebrandt, L. Bruckner-Tuderman, G.F. Laube, Integrin alpha3 mutations with kidney, lung, and skin disease, N. Engl. J. Med. 366 (16) (2012) 1508–1514.

[30] N. Sachs, M. Kreft, M.A. van den Bergh Weerman, A.J. Beynon, T.A. Peters, J.J. Weening, A. Sonnenberg, Kidney failure in mice lacking the tetraspanin CD151, J. Cell Biol. 175 (1) (2006) 33–39.

[31] R.M. Baleato, P.L. Guthrie, M.C. Gubler, L.K. Ashman, S. Roselli, Deletion of CD151 results in a strain-dependent glomerular disease due to severe alterations of the glomerular basement membrane, Am. J. Pathol. 173 (4) (2008) 927–937.

[32] J.D. Fine, R.A. Eady, E.A. Bauer, R.A. Briggaman, L. Bruckner-Tuderman, A. Christiano, A. Heagerty, H. Hintner, M.F. Jonkman, J. McGrath, J. McGuire, A. Moshell, H. Shimizu, G. Tadini, J. Uitto, Revised classification system for inherited epidermolysis bullosa: report of the Second International Consensus Meeting on Diagnosis and Classification of Epidermolysis Bullosa, J. Am. Acad. Dermatol. 42 (6) (2000) 1051–1066.

[33] J.D. Fine, R.A. Eady, E.A. Bauer, J.W. Bauer, L. Bruckner-Tuderman, A. Heagerty, H. Hintner, A. Hovnanian, M.F. Jonkman, I. Leigh, J.A. McGrath, J.E. Mellerio, D.F. Murrell, H. Shimizu, J. Uitto, A. Vahlquist, D. Woodley, G. Zambruno, The classification of inherited epidermolysis bullosa (EB): report of the Third International Consensus Meeting on Diagnosis and Classification of EB, J. Am. Acad. Dermatol. 58 (6) (2008) 931–950.

[34] Z. Lin, S. Li, C. Feng, S. Yang, H. Wang, D. Ma, J. Zhang, M. Gou, D. Bu, T. Zhang, X. Kong, X. Wang, O. Sarig, Y. Ren, L. Dai, H. Liu, J. Zhang, F. Li, Y. Hu, G. Padalon-Brauch, D. Vodo, F. Zhou, T. Chen, H. Deng, E. Sprecher, Y. Yang, X. Tan, Stabilizing mutations of KLHL24 ubiquitin ligase cause loss of keratin 14 and human skin fragility, Nat. Genet. 48 (12) (2016) 1508–1516.

[35] Y. He, K. Maier, J. Leppert, I. Hausser, A. Schwieger-Briel, L. Weibel, M. Theiler, D. Kiritsi, H. Busch, M. Boerries, K. Hannula-Jouppi, H. Heikkila, K. Tasanen, D. Castiglia, G. Zambruno, C. Has, Monoallelic mutations in the translation initiation codon of KLHL24 cause skin fragility, Am. J. Hum. Genet. 99 (6) (2016) 1395–1404.

[36] S. Richards, N. Aziz, S. Bale, D. Bick, S. Das, J. Gastier-Foster, W.W. Grody, M. Hegde, E. Lyon, E. Spector, K. Voelkerding, H.L. Rehm, A.L.Q.A. Committee, Standards and guidelines for the interpretation of sequence variants: a joint consensus recommendation of the American College of Medical Genetics and Genomics and the Association for Molecular Pathology, Genet. Med. 17 (5) (2015) 405–424.

[37] A. Dobin, C.A. Davis, F. Schlesinger, J. Drenkow, C. Zaleski, S. Jha, P. Batut, M. Chaisson, T.R. Gingeras, STAR: ultrafast universal RNA-seq aligner, Bioinformatics 29 (1) (2013) 15–21.

[38] E.C. Figueira, D.F. Murrell, M.T. Coroneo, Ophthalmic involvement in inherited epidermolysis bullosa, Dermatol. Clin. 28 (1) (2010) 143–152.

[39] J.D. Fine, L.B. Johnson, M. Weiner, A. Stein, S. Cash, J. Deleoz, D.T. Devries, C. Suchindran, Eye involvement in inherited epidermolysis bullosa: experience of the National Epidermolysis Bullosa Registry, Am J. Ophthalmol. 138 (2) (2004) 254–262.

[40] J.T. Wright, Oral manifestations in the epidermolysis bullosa spectrum, Dermatol. Clin. 28 (1) (2010) 159–164.

[41] J.D. Fine, J.E. Mellerio, Extracutaneous manifestations and complications of inherited epidermolysis bullosa: part I. Epithelial associated tissues, J. Am. Acad. Dermatol. 61 (3) (2009) 367–384 (quiz 385-6).

[42] L. Bruckner-Tuderman, Dystrophic epidermolysis bullosa: pathogenesis and clinical features, Dermatol. Clin. 28 (1) (2010) 107–114.

[43] N. Kambham, N. Tanji, R.L. Seigle, G.S. Markowitz, L. Pulkkinen, J. Uitto, V.D. D'Agati, Congenital focal segmental glomerulosclerosis associated with beta4 integrin mutation and epidermolysis bullosa, Am. J. Kidney Dis. 36 (1) (2000) 190–196.

[44] K. Kaneko, M. Kakuta, Y. Ohtomo, T. Shimizu, Y. Yamashiro, H. Ogawa, M. Manabe, Renal amyloidosis in recessive dystrophic epidermolysis bullosa, Dermatology 200 (3) (2000) 209–212.